Materials Research Proceedings 41 (2024) 2554-2561 https://doi.org/10.21741/9781644903131-281

Optimizing powder compaction for enhanced relative density: Insights from multi-particle finite element simulations and genetic algorithm

GHORBANI-MENGHARI Hossein[1,a], KIM Hwi-Jun[2,b], CHOI Hyunjoo[3,c], CHA Pil-Ryung[3,d] and KIM Ji Hoon[1,e*]

[1]School of Mechanical Engineering, Pusan National University, South Korea

[2]Korea Institute of Industrial Technology, Incheon, South Korea

[3]School of Advanced Materials Engineering, Kookmin University, Seoul, South Korea

[a]en.ghorbani@gmail.com, [b]khj@kitech.re.kr, [c]hyunjoo@kookmin.ac.kr, [d]cprdream@kookmin.ac.kr, [e]kimjh@pusan.ac.kr

Keywords: Powder Compaction, Element Number Per Particle, Particle Size Distribution, Multi-Particle Finite Element Modeling

Abstract. In this study, multi-particle finite element simulations in powder compaction were performed to analyze the effects of the size of the representative volume element (RVE), the number of elements per particle, and particle size distribution. Simulation parameters were calibrated to accurately predict the relative density of compacts derived from two types of powders. The influence of RVE size across four mixtures was examined to obtain its relationship with relative density. The impacts of particle size distribution and element number per particle were studied. The results indicate a decline in relative density with increased element size. Moreover, a genetic algorithm is employed to determine the optimum mixture composition yielding the highest relative density at 1400 MPa.

Introduction

Powder compaction is a manufacturing process used to shape powdered materials into a desired form by applying pressure. This process is widely employed in industries such as powder metallurgy, pharmaceuticals, ceramics, and cosmetics, among others. The primary goal of powder compaction is to transform a loose powder into a solid, dense product with specific geometrical and mechanical properties.

The final characteristics of tablets are primarily influenced by stresses on the powder during compaction. Factors affecting this stress can directly alter tablet outcomes. The study by Mazel et al. [1] examined the role of friction between tooling and powder on die-wall pressure during compaction, using both flat and concave punches. Tests were conducted on microcrystalline cellulose, complemented by finite element method (FEM) simulations. Both approaches showed that increased friction leads to a rise in die-wall pressure, a finding contrasting some existing literature. For flat punches, the stress changes were influenced mainly by die-powder friction. However, with concave punches, friction alterations between punches and powder also impacted die-wall pressure, which is relevant in scenarios where friction changes due to film deposits on punches. The densification of Cu–Al mixed metal powder in double-action die compaction was studied through numerical modeling by Wang et al. [2]. Comparisons were made between single-action and double-action compaction, with the latter enhancing densification, aligning with the Van Der Zwan–Siskens equation. Different initial packing structures showed that denser setups resulted in better compacts. The compact density rose as Al content increased, but stress dropped. Conversely, with consistent Al content, increased compaction pressures raised both density and stress. The impact of friction on compaction was evident in its effect on powder flow and stress

distribution. Extended dwell times aided densification, while a larger height-to-diameter ratio impeded it. Compacting powders at high loads is challenging due to particle movement and breakage. While tableting is critical in pharmaceuticals, a deeper connection between large-scale powder behavior and micro-properties is sought. Using a compaction simulator, Cabiscol et al. [3] studied the behavior of limestone powders under different pressures. The compatibility of limestone was analyzed using the traditional Heckel model and the newer Wünsch model, with the latter showing enhanced adaptability. High-pressure results revealed that the role of large particle interlocking, evident at lower pressures, diminishes. Notably, tablet strength remained consistent for particles with a median size below 10 μm, but for larger particles, strength reduced as size increased. Binder jetting additive manufacturing (AM) offers a cost-effective way to create intricate metal parts, but achieving total density without notable sintering shrinkage is challenging. To address this, Bai et al. [4] studied bimodal powder mixtures in binder jetting copper. The results showed that compared to using uniform fine powders, bimodal mixtures increased packing density by 8.2% and sintered density by 4.0% while improving flowability by 10.5% and reducing sintering shrinkage by 6.4%.

In this study, multi-particle finite element simulations in powder compaction were performed to analyze the effects of the size of the representative volume element (RVE), the number of elements per particle, and particle size distribution. Simulation parameters were calibrated to accurately predict the relative density of compacts derived from two types of powders. The influence of RVE size across four mixtures was examined to obtain its relationship with relative density. The impacts of particle size distribution and element number per particle were studied. The results indicate a decline in relative density with increased element size.

Material Property

In this study, the powder under investigation consists of Fe-Si-Al-P. The modeling approach involves implementing a parametric Python script to generate random particles and simulate the powder compaction process. The simulation is conducted using the dynamic explicit analysis, allowing for a comprehensive exploration of the compaction dynamics. Compression testing was executed using the Instron 8501 Servo Hydraulic Machine, which utilizes a servo-regulated hydraulic mechanism to exert compressive forces on specimens. Table 1 illustrates the material characteristics of this model.

Table 1 Material properties.

Parameter	Value
Elastic modulus [GPa]	170
Poisson's ratio	0.3
ρ (kg/m^3)	7,130

To accurately capture the material behavior during compaction, the stress-strain curve is fitted using a power law Swift hardening model, expressed as $\sigma=K(\varepsilon+\varepsilon 0)m$. The power law Swift parameters are set as follows: K (material constant) is assigned a value of 1380, m (strain hardening exponent) is determined to be 0.245, and ε_0 (initial strain) is specified as 0.0354. Fig. 1 illustrates the Stress-strain curve of the Fe-Si-Al-P alloy powder.

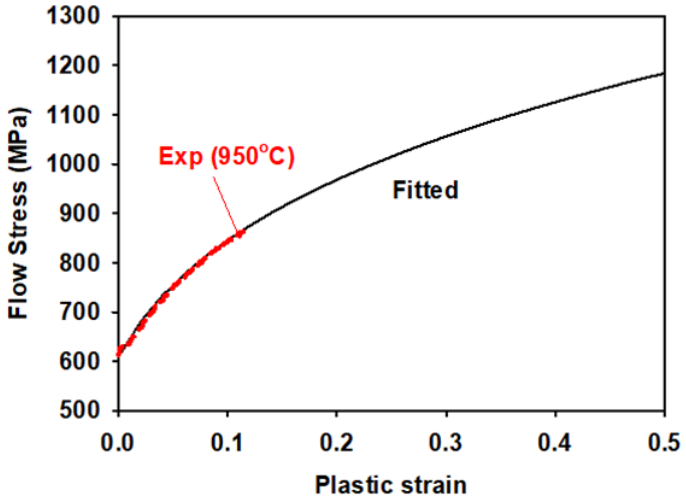

Fig. 1 Stress-strain curve of the Fe-Si-Al-P alloy powder

Multi-Particle Finite Element Model

In this approach, each particle is individually depicted as a solid component and is discretized using the four-node tetrahedral elements (C3D4). Providing a fine mesh is important for thoroughly analysing particle behavior during compaction. Meanwhile, the punch and die are other components represented as discrete 3D rigid bodies.

Generating the RVE is a crucial step in ensuring the accuracy of the simulation. A customized MATLAB code [5,6], complemented by a Python script, was developed. The goal was to create a realistic representation of each particle fully encapsulated by the die. The initial relative density of the RVE is set at 40 percent. This parameter is essential for accurately reflecting the initial state of the powder and has implications for the subsequent compaction behavior. Furthermore, special attention is given to the composition of the RVE. It is essential that the RVE composition accurately mirrors the proportions of fine to coarse particles in the actual powder system. Achieving this accurate representation is crucial for capturing the diverse characteristics of the powder mixture and simulating the compaction process with a high degree of fidelity. Fig. 2 shows the generated particles and die.

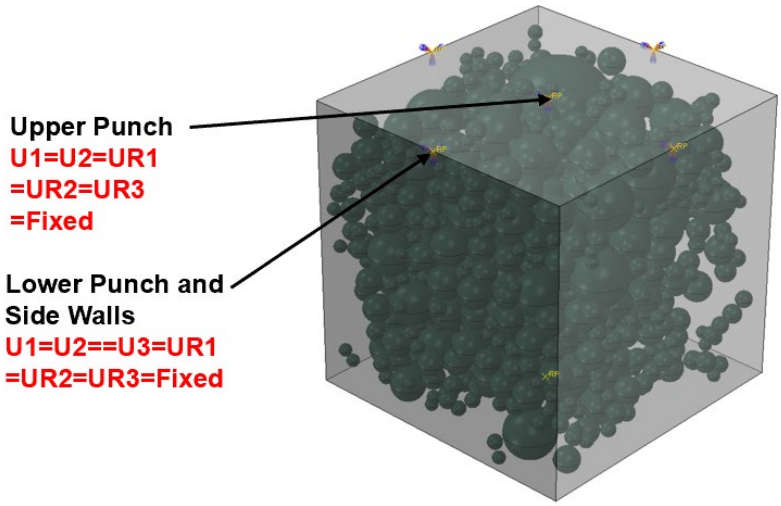

Fig. 2 3D MPFEM model implemented in Abaqus for [75,25] mixture

Results and Discussion

Influence of element size on the relative density. In examining the influence of the number of elements per particle on the relative density within the context of powder compaction, a 3D linear tetrahedral element (C3D4) Finite Element (FE) model was employed. The powder system, characterized by a particle diameter of 125.5 μm, was simulated within an RVE measuring 1200x1200x1200 μm³ and comprising 507 particles. A range of element sizes, determined by varying seed sizes, was investigated, leading to distinct elements per particle (Elem/Particle) ratios and corresponding edge lengths. Notably, as the Elem/Particle increased—from 26 for a seed size of 1000 μm to 2252 for a seed size of 15 μm—a discernible trend emerged: a consistent rise in relative density. This suggests that finer discretization, reflected in higher Elem/Particle ratios, plays a crucial role in enhancing the accuracy of the simulation, enabling a more precise representation of the powder compaction process. These findings underscore the importance of carefully selecting the element size to balance computational efficiency, and ensuring the accuracy of results in simulations of powder compaction is crucial. Fig. 3 depicts the influence of element/particle on the relative density.

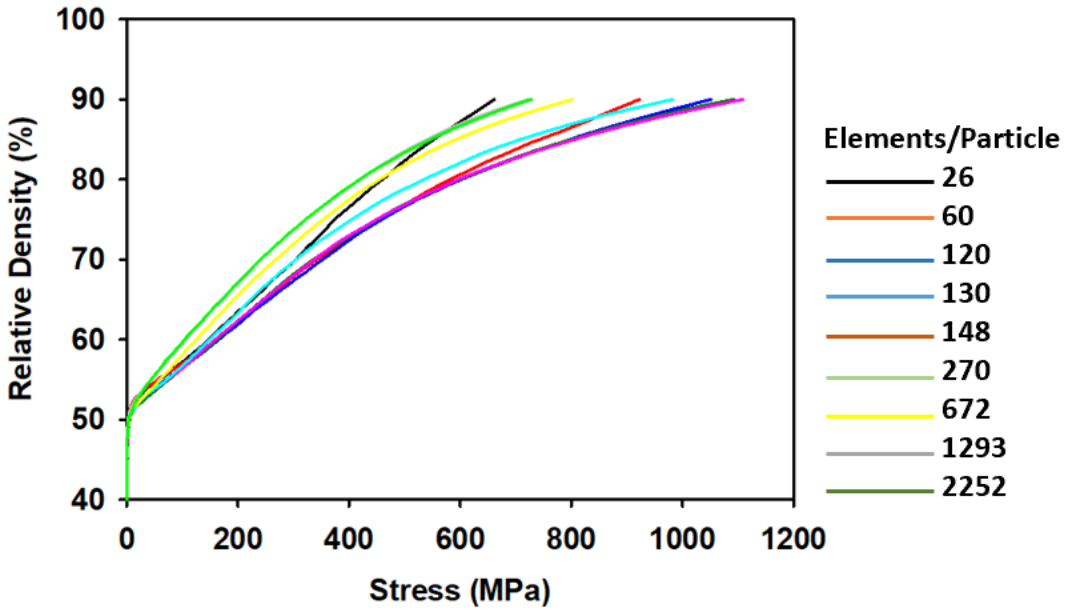

Fig. 3 The influence of elements/particles on the relative density.

Effect of RVE Size on the Relative Density. The influence of the RVE size on the relative density was analyzed. RVE sizes of 240, 305, and 350 micrometers for the [50,50] mixture were considered. Fig. 4 illustrates the impact of RVE size on relative density for the [50,50] mixtures. Increasing the RVE size results in a corresponding increase in initial density. However, it is essential to note that while this variation becomes more significant at lower pressures, the difference decreases and becomes relatively insignificant in areas where higher pressures are applied.

Effect of Particle Size Distribution on the Relative Density. To investigate the influence of particle size distribution on relative density, experimental tests with four distinct mixtures were conducted: [0,100], [25,75], [75,25], and [100,0], where the first number represents the percentage of fine particles and the second denotes the percentage of coarse particles. Fig. 5 demonstrates the relationship between pressure and relative density for various particle size distributions. As evident from Fig. 5, the relative density of pure particles—fine or coarse—is notably lower than the rest of the mixtures. Among the mixtures, the [0,100] composition exhibits the lowest relative density, surpassing even the [100,0] mixture. Notably, when comparing the [75,25] and [25,75] mixtures,

[75,25] stands out with the highest relative density, particularly at lower pressure levels. However, as pressure increases, the distinction in relative density between [75,25] and [25,75] diminishes, becoming relatively insignificant. This behavior is intricately tied to the plastic deformation of particles, with coarse particles experiencing less plastic deformation than fine particles. The result is greater elastic recovery, especially at lower pressures, contributing to the observed variations in relative density across different mixtures.

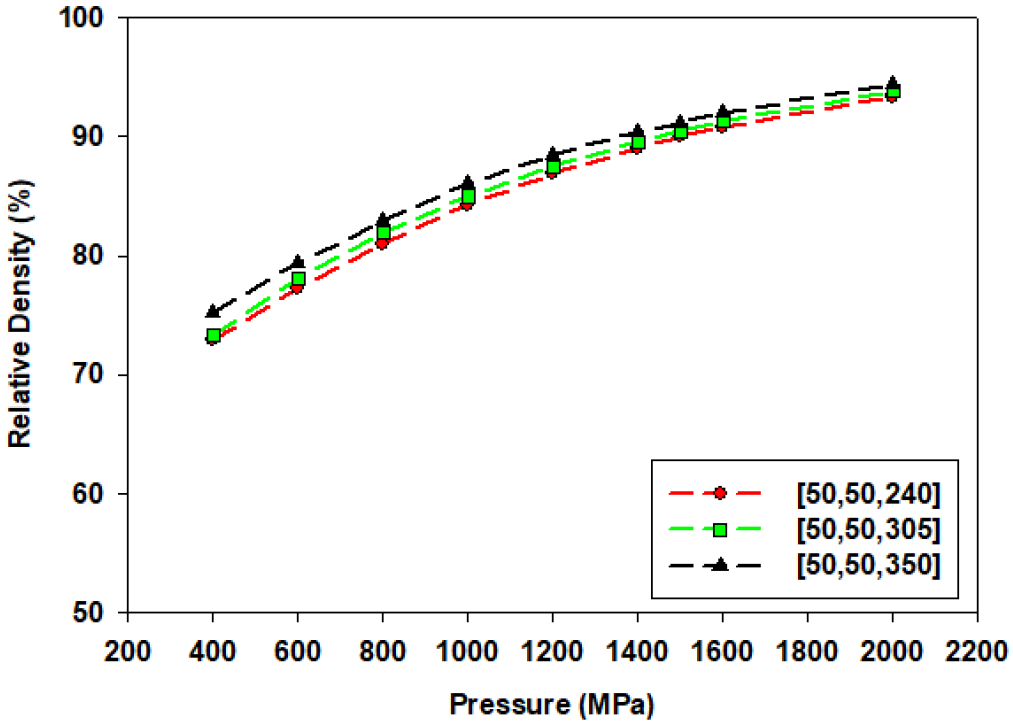

Fig. 4 Effect of RVE size on the relative density for [50,50]

Fig. 6 illustrates a relative density comparison between EXP and MPFEM at 1600 MPa. The results obtained from MPFEM closely align with the experimental findings, demonstrating a similar trend. This consistency in trends between the simulation and experimental data reinforces the reliability of the MPFEM results in capturing the relative density behavior during loading at 1600 MPa.

Finding the Optimum Mixture with the highest Relative Density Using a Genetic Algorithm. Genetic Algorithms (GAs), inspired by natural selection and genetics, offer a robust approach to solving complex optimization problems [7]. The GA procedure involves several key steps:

1. Initial Population:
    - Generate a set of potential solutions represented by chromosomes, $P=\{p_1, p_2,\ldots,p_s\}$, consisting of random real values.
2. Evaluation (Fitness Calculation):
    - Define a fitness function, $g(P)$, to assess the performance of each chromosome in the population based on the optimization objective.
3. Selection:
    - Arrange chromosomes by their fitness values.
    - Select two parents for crossover and mutation based on their fitness.

4. Genetic Operators:
    - Create new chromosomes or offspring (C_1 and C_2), from the selected parents using genetic operators.
5. Crossover:
    - Exchange information between two parents to generate new offspring.
6. Mutation:
    - Introduce changes to the genes of the crossed offspring chromosomes.

This iterative process continues until a convergence criterion is met or a specified number of generations is reached. The GA aims to explore the solution space efficiently, providing a robust methodology for determining the optimum mixture composition that yields the highest relative density at 1400 MPa.

$$\begin{gathered} \text{maximize} \quad F(M) = Obj_s\,(m_1, m_2\,) \\ 0 \le m_1 \le 100 \\ 0 \le m_2 \le 100 \\ m_1 + m_2 = 100 \end{gathered}$$

where m_1 and m_2 represent the volume fractions of the two powders, $F(M)$ is the maximum relative density as the objective function at 1400 MPa. Table 2 illustrates the optimum mixture with the highest relative density at 1400 MPa.

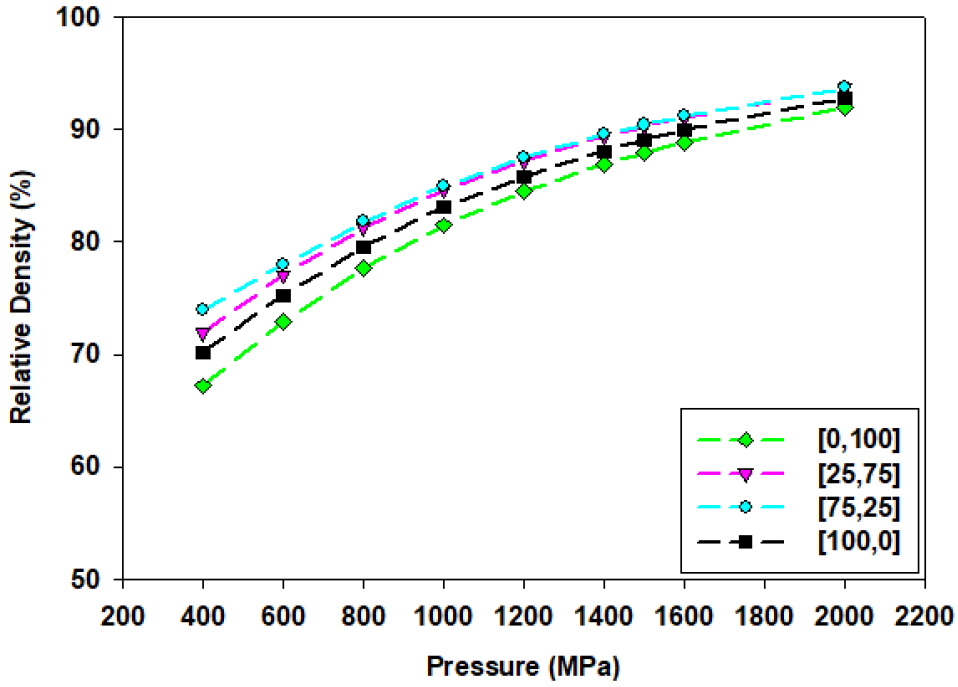

Fig. 5 Relative density for various particle size distributions

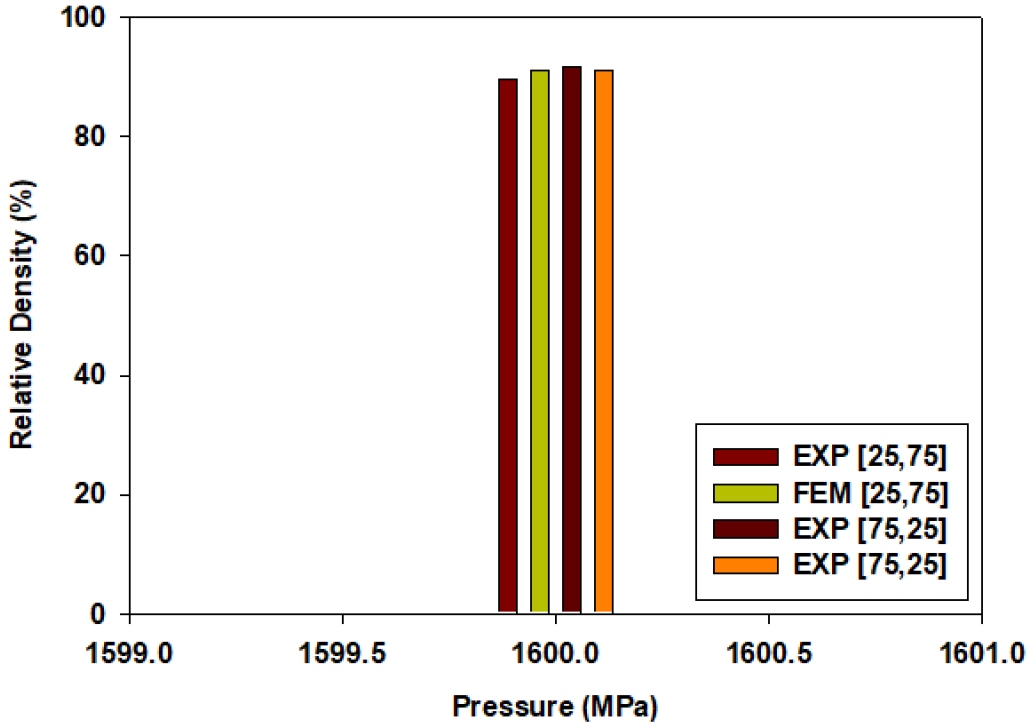

Fig. 6 Relative density comparison within EXP and MPFEM at 1600 MPa

Table 2 The optimum mixture with the highest relative density at 1400 MPa

Mixture [Fine, Coarse]	[66.74, 33.26]
Relative Density	85.6107

Conclusion

This study explored the intricate details of powder compaction through advanced simulation techniques and optimization algorithms. The objective was to fine-tune simulation parameters to accurately predict the relative density of compacts derived from two types of powders. Key findings include the significant impact of element size, RVE size, and particle distribution on relative density. The delicate balance between these factors is crucial in accurately predicting the compaction process. Using a genetic algorithm to identify the optimum mixture composition for maximum relative density at 1400 MPa further demonstrates the potential for advanced optimization techniques in powder compaction studies. These insights contribute to the evolving understanding of powder compaction dynamics and offer valuable guidance for optimizing the process in various industrial applications.

References

[1] V. Mazel, H. Diarra, P. Tchoreloff, Effect of friction between powder and tooling on the die-wall pressure evolution during tableting: Experimental and numerical results for flat and concave punches, Int. J. Pharma, 554 (2019) 116-124. https://doi.org/10.1016/j.ijpharm.2018.11.003

[2] W. Wang, H. Qi, P. Liu, Y. Zhao, H. Chang, Numerical simulation of densification of cu–al mixed metal powder during axial compaction, Int. J. Metals. 8 (2018) 537. https://doi.org/10.3390/met8070537

[3] R. Cabiscol, H. Shi, I. Wünsch, V. Magnanimo, J.H. Finke, S. Luding, A. Kwade, Effect of particle size on powder compaction and tablet strength using limestone, Int. J. Adv. Powder. Tech. 31 (2020) 1280-1289. https://doi.org/10.1016/j.apt.2019.12.033

[4] Y. Bai, G. Wagner, C.B. Williams, Effect of particle size distribution on powder packing and sintering in binder jetting additive manufacturing of metals, Int. J. Manuf. Sci. Eng. 139 (2017) 081019. https://doi.org/10.1115/1.4036640

[5] P. Kahhal, H. Ghorbani-Menghari, H.J. Kim, H. Choi, P.R. Cha, J.H. Kim, Metaheuristic optimization of powder size distribution in powder forming process using multi-particle finite element method coupled with artificial neural network and genetic algorithm, J. Mater. Trans. 64 (2023) 2648-2655. https://doi.org/10.2320/matertrans.MT-MI2022006

[6] P. Kahhal, J. Jung, Y.C. Hur, Y.H. Moon, J.H. Kim, Analysis of powder compaction process using multi-particle finite element method, J. Mater. Trans. 63 (2022) 1576-1582. https://doi.org/10.2320/matertrans.MT-MB2022012

[7] R.B. Carmona-Paredes, R. Domínguez-Mora, M.L. Arganis-Juárez, M.L., E. Juan-Diego, R. Mendoza-Ramírez, E. Carrizosa-Elizondo, use of evolutionary computation and guide curves to optimize the operating policies of a reservoir system established to supply drinking water, J. Appl. Water. Sci. 13 (2023) 2. https://doi.org/10.1007/s13201-022-01807-z